

geofísica
internacional

Geofísica Internacional

ISSN: 0016-7169

silvia@geofisica.unam.mx

Universidad Nacional Autónoma de México
México

Dasso, S.; Gopalswamy, N.; Lara, A.
Forecast of solar ejecta arrival at 1 AU from radial speed
Geofísica Internacional, vol. 43, núm. 1, january-march, 2004, pp. 47-52
Universidad Nacional Autónoma de México
Distrito Federal, México

Available in: <http://www.redalyc.org/articulo.oa?id=56843107>

- How to cite
- Complete issue
- More information about this article
- Journal's homepage in redalyc.org

redalyc.org

Scientific Information System
Network of Scientific Journals from Latin America, the Caribbean, Spain and Portugal
Non-profit academic project, developed under the open access initiative

Forecast of solar ejecta arrival at 1 AU from radial speed

S. Dasso^{1,2}, N. Gopalswamy¹ and A. Lara³

¹ NASA/Goddard Space Flight Center, Greenbelt, MD, and Center for Solar Physics and Space Weather, The Catholic University of America, Washington DC, USA

² Present Address: Instituto de Astronomía y Física del Espacio (IAFE), Buenos Aires, Argentina

³ Instituto de Geofísica, UNAM, Mexico

Received: March 31, 2001; accepted: October 14, 2002

RESUMEN

Las eyecciones transitorias de masa solar (EMS) pueden producir cambios en el campo geomagnético. Cuando la polaridad magnética de la EMS es adecuada, puede disparar intensas tormentas geomagnéticas. La predicción de la llegada de EMS desde el Sol al geoespacio tiene una importancia crucial para poder predecir el clima espacial. En este trabajo implementamos un modelo simple, desarrollado por Gopalswamy *et al.*, 2000 para estimar el tiempo de llegada de EMS a una Unidad Astronómica. Este modelo requiere sólo un parámetro de entrada: la velocidad radial de la EMS en el momento de su expulsión desde el Sol. Cuando la velocidad de la EMS es medida desde una posición dentro de la línea Sol-Tierra, sólo la componente de la velocidad en el plano del cielo puede ser obtenida. Debido a que la predicción del modelo depende de la velocidad inicial de la EMS observada remotamente, es muy importante obtener esta velocidad lo más exactamente posible. Una de las mayores incertezas cuando se mide la velocidad inicial de la EMS es el efecto de proyección. El objetivo de este trabajo es corregir efectos de proyección a partir de la localización en la superficie solar de la erupción y del tamaño de apertura de la EMS. Encontramos que la corrección desarrollada acuerda con un modelo obtenido en observaciones estereoscópicas en el pasado.

PALABRAS CLAVE: Eyección de masa coronal, clima espacial, nubes magnéticas, tormentas geomagnéticas.

ABSTRACT

Solar ejecta produce changes in the interplanetary magnetic field of the terrestrial environment. When the magnetic polarity of the ejecta is suitable, it may trigger intense geomagnetic storms. Therefore, prediction of the arrival of solar ejecta in the geospace is of crucial importance for space weather applications. We implement a simple model, developed by Gopalswamy *et al.*, (2000) to estimate the time of arrival for solar ejecta at 1AU. This model requires just one input parameter: the radial speed of the associated coronal mass ejection (CME) at the moment of its expulsion from the Sun. When the speed of the CME is measured from a location on the Sun-Earth line, only the plane of the sky speed can be obtained. Since the prediction model depends on the initial speed of the CMEs observed remotely, it is important to obtain this speed as accurately as possible. One of the major uncertainties in the measured initial speed is the extent of projection effects. We attempt to correct for projection effects using the solar surface location of the eruption and assuming a width to the CME. We found that the correction is in agreement with a model obtained from stereoscopic observations from the past.

KEY WORDS: Coronal mass ejection, space weather, magnetic clouds, geomagnetic storms.

INTRODUCTION

Interplanetary ejecta with a southward oriented magnetic field are known to trigger intense geomagnetic perturbations (Dungey 1961; Gonzalez *et al.*, 1998; Cane *et al.*, 2000) as a consequence of reconnection processes taking place between the ejecta field and the geomagnetic field. Other interplanetary entities such as shocks and solar energetic particles are also geoeffective, but these are also caused by CMEs. For instance some special class of shocks can be observed at the surroundings of Earth without obvious drivers behind them, however they are associated with coronal mass ejections (CMEs) expelled in the direction perpendicular to the Sun-Earth line (Gopalswamy *et al.*, 2001). Thus,

CMEs are of fundamental importance and the prediction of their 1-AU arrival time is one of the major requirements to forecast the space weather conditions in the terrestrial environment.

Several authors have developed models in order to study the dynamic of CMEs through the interplanetary medium, including propelling and drag forces (see e.g., Farrugia *et al.*, 1993; Osherovich *et al.*, 1993; Cargill *et al.*, 1995; Yeh, 1995; and Chen, 1997). Most of these models consider several interplanetary properties, such as the background solar wind speed, and the density of the ejecta. However, only a few measurements are available to us when the CME is near the Sun: the projection of the speed on the plane of the sky

(observed remotely using white light coronagraphs such as SOHO-LASCO) and the estimation of the angular position of the ejection (observed also remotely such as analysing H_α emission). The model developed by Gopalswamy *et al.* (2000) to estimate the arrival time of CMEs is implemented here, but considering geometrical corrections in order to obtain the radial speed (u_r) of the CME from the observed sky-plane speed (u_s). The model assumes that the motion of the object is with a constant acceleration, equal to its average effective acceleration, and makes use of the strong correlation observed between the effective acceleration and its initial speed. In Section 2 we show the importance of projection effects and attempt correct for them for a set of CME events. In Section 3, we compare our results with a model to predict the time of travel of ejecta. Finally we present our conclusions in Section 4.

GEOMETRICAL CORRECTION

In the first part of this section we describe briefly how we calculate the radial speed (u_r) of the CME from the projection of the sky plane speed (u_s) of the CME, and the angular position of the source region, from where the CME is expelled. In the second part, we determine the ratio u_r/u_s for our set of events. The speed u_s is measured from the remote observation of consecutive positions of the CME front. The three LASCO coronagraphs (C1, C2, and C3) on board the spacecraft SOHO have a combined field of view, which includes a significant range of radial distance from the solar disk center. They cover distances from $\sim 1.2R_s$ to $\sim 32R_s$. Then, assuming that the CME proceeds radially outward from some point near the solar surface (i.e., $r=R_s$), it is possible to obtain u_r from geometry (Sheeley *et al.*, 1999; Leblanc *et al.*, 2001). In this work, we estimate the angular position of the CME source (i.e., the latitude = λ and the longitude = ψ) as the active region (AR) position.

Under the assumption of a radial expulsion of the CME from the AR, the angle (ϕ) between the Earth-Sun direction and the radial passing through the AR, is very useful in order to determine the radial speed. The magnitude of ϕ can be simply obtained from λ and ψ as:

$$\cos(\phi) = \cos(\lambda) \cos(\psi). \quad (1)$$

By the other hand, we assume the same model as LeBlanc *et al.* (2001), where the evolution of the CME is modeled with an expanding circular front, with a fixed angle between the legs. The angle between the legs defines a cone with its vertex in the AR, and with an opening semi-angle (α_r).

When it is possible, α_r can be obtained from direct observations of the width of the CME. While it is easy to mea-

sure the width for limb CMEs (those ejected in the sky plane), it is impossible to measure width for halo CMEs we are interested in. In fact the apparent width of geoeffective CMEs is often 360 degrees, which is obviously not related to the CME cone angle.

The relation between u_r and u_s has been derived by LeBlanc *et al.* [2001] as,

$$u_r = u_s (1 + \sin \alpha_r) / (\sin \phi + \sin \alpha_r). \quad (2)$$

From the observed heliographic location of the CME source, we can obtain ϕ . However, we have to use α_r as a parameter to estimate the correction factor. Figure 1 shows the ratio u_r/u_s , from Eq. 2, for ϕ ranging from 0 to 90 degrees, for different values of α_r . First of all, we note that for events with $\phi > 60^\circ$ there is no projection effect, as expected. The limb events are less likely to be geoeffective. However for disk events (low values of ϕ), which are likely to be geoeffective, the projection effect is large, reaching values of u_r/u_s from 1.6 to 2.3 when ϕ is 20° and α_r is between 10° and 60° . Note also that the projection effect is more important for narrow CMEs (small α_r). For $\alpha_r \sim 15^\circ$ and $\phi \sim 10^\circ$, it is possible to reach $u_r/u_s \sim 3$, but for the same position of the CME ejection, $u_r/u_s \sim 1.8$ for $\alpha_r \sim 60^\circ$. CMEs in general have a broad distribution of widths (St Cyr *et al.*, 2000; Gopalswamy *et al.*, 2001) so it is difficult to choose an angular width for each one of the CMEs. This is a major difficulty in applying projection corrections.

CORRECTION TO A SET OF OBSERVED SPEEDS

In this paper we analyze 20 of the 23 events studied in (Gopalswamy *et al.*, 2000). We exclude three events because either the information on their source position is not available, or the identification of the interplanetary manifestation of the CME is uncertain. For each event we know the latitude (λ) and the longitude (ψ) of the source region of the CME, the initial speed observed by LASCO (u_s), the speed of the associated interplanetary ejecta at 1 AU (V_{ej}) observed by the Wind spacecraft, the transit time (τ), and the apparent opening angle of the cone of the CME (the width) seen on the plane of the sky.

The events are numbered in chronological order in Figure 2 with the stars of indicating u_s versus the event number. The vertical bar above each event indicates the range of possible values for u_r , according to Eq. (2), using the measured value for ϕ (from λ , ψ , and Eq. (1)), and changing the values of α_r from 10° to 60° . Thus, $\alpha_r = 10^\circ$ determines the top of the bar, while $\alpha_r = 60^\circ$ determines the bottom. Note that u_r and u_s differ significantly for most of the CMEs for all the values of α_r considered. The X (diamond) symbols on the bars denote the values of u_r when $\alpha_r = 36^\circ$ ($\alpha_r = 45^\circ$). The

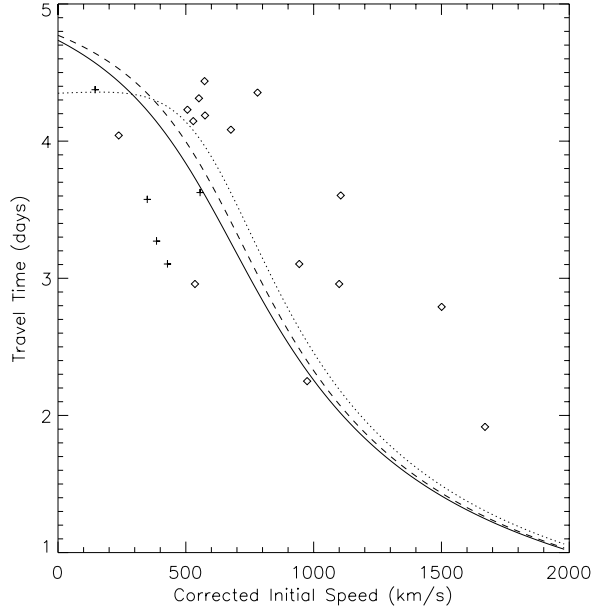


Fig. 1. Corrected to uncorrected velocity ratio versus the angle between the radial direction of the CME and the Sun-Earth direction. Different curves show different (fixed) values for the semi-angle of the cone (α_r).

opening semi-angle $\alpha_r = 36^\circ$ is statistically the most frequent value (St. Cyr *et al.*, 2000). For instance for the event number 18, u_s is 1044 km/s, but the corrected speed (assuming $\alpha_r = 36^\circ$) is $u_r = 1749$ km/s, a huge difference of 705 km/s (almost a 70% of the measured velocity).

An apparent width greater than 180° is observed in the 80% of the events. For these cases α_r can not be obtained from a simple projection. However, Figure 2 shows that u_r/u_s is not very sensitive to α_r , for α_r between 36° and 45° . In order to perform a first correction to the plane of the sky speed, we assume that $\alpha_r = 45^\circ$ for all the events. Note that our assumption is a bit more moderate than lower values of α_r (i.e., take $\alpha_r = 45^\circ$ correct a bit less the initial speed than take $\alpha_r = 36^\circ$). Several other criteria have been explored in order to assign values to α_r , but all of them yielded similar results.

As was shown by Gopalswamy *et al.* (2000), the plane of the sky speed (near the Sun) and the effective acceleration, $a_s = (V_{ej} - u_s) / \tau$, are well correlated. When a linear fit to the $a_s - u_s$ plot yields, $a_s = -0.0034u_s + 1.36$; here a_s is expressed in m/s^2 and u_s in km/s. If we set $a = 0$, a critical velocity of $\hat{u}_s = 399.4$ km/s is obtained.

In order to avoid the projection effects, Gopalswamy *et al.* (2002a) analyzed pairs of CME-IP ejecta using data from the Solwind coronagraph on board P78-1 (remote sens-

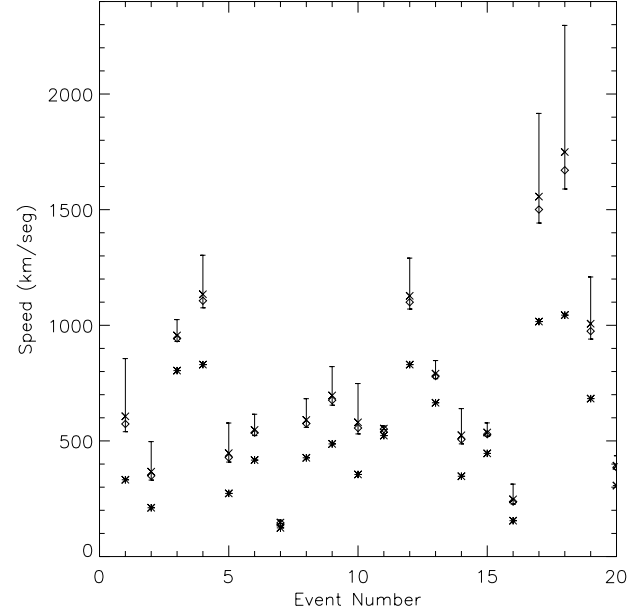


Fig. 2. Speed versus number of the case. Stars correspond to the uncorrected speeds. For a given event, bars show the range of possible values to u_r , from Eq. (2) and considering $\alpha_r \in (10^\circ, 60^\circ)$. Rhombuses and X represent u_r for $\alpha_r = 45^\circ$ and $\alpha_r = 36^\circ$, respectively.

ing) and from Pioneer Venus Orbiter (PVO) and Helios 1 (*in situ* measurements). The projection effect is minimized because the remote-sensing and *in situ* spacecraft were in quadrature. They found that the empirical relationship between the initial speed and the effective acceleration was maintained with the same functional form but with slightly different coefficients: $a_{PVO-Helios1} = -0.0043u + 1.77$. The resulting critical speed was $\hat{u}_{PVO-Helios1} = 411.4$ km/s.

When the effective acceleration is calculated from the list of events studied in this paper (SOHO-Wind, using u_r instead u_s) $a_r = (V_{ej} - u_r) / \tau$, the high correlation remains between a_r and u_r . From a straight line fit, we obtain $a_r = -0.0042u_r + 1.79$, a very similar result to that obtained with PVO-Helios1 in a way totally independent and without any projection effect.

The acceleration versus the initial speed is shown in Figure 3; the stars show accelerations from the uncorrected speeds, while diamonds are used for the radial case. The dotted straight line represents the fit obtained from (u_s, a_s) , and the solid line corresponds to the fit for (u_r, a_r) . The fit obtained with PVO-Helios1 data (Gopalswamy *et al.*, 2002) are also shown (dashed line). When α_r is decreased, the slope of the solid straight line slightly decreases, i.e., the absolute value of the acceleration slightly increases. However when $\alpha_r = 36^\circ$, a very similar result is obtained.

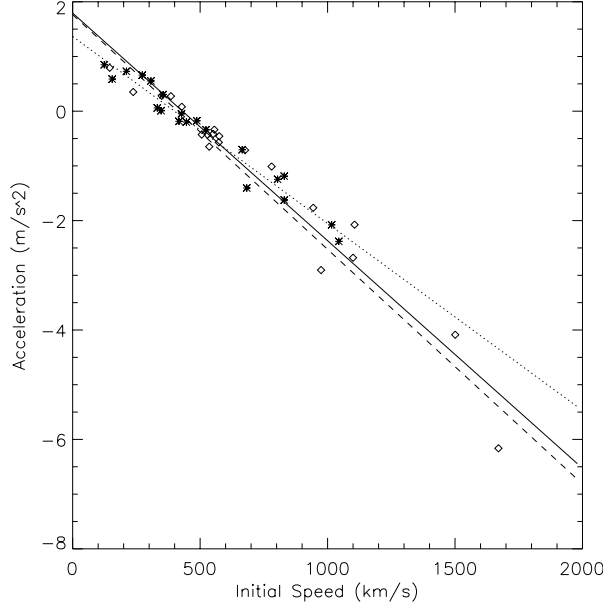


Fig. 3. Acceleration versus initial speed. Stars and rhombuses correspond to uncorrected and corrected (assuming $\alpha_r=45^\circ$ in the last case) speed, respectively. The dotted, solid, and dashed straight lines show the fit considering stars, rhombuses, and PVO-Helios1 data (points not shown).

Figure 4 shows the speed of the ejecta at 1AU (V_{ej}) versus u_r . While the correlation between V_{ej} and u_s is 0.61, a slightly better correlation (0.67) is obtained when the corrected speed is considered. It is also possible to differentiate a group of CMEs (marked with pluses) which do not seem to be ordered with the same law as the rest of the events. We can speculate about that the stars events belong to a potential second class of CMEs (Sheeley *et al.*, 1999). The value of the correlation between V_{ej} and u_r (u_s) is 0.89 (0.83) when these 5 events are not considered.

From a model considering an effective constant acceleration, i.e., $a_{ef} = (V_{ej} - u_r)/\tau$, (Gopalswamy *et al.*, 2000), and making use of the empirical linear dependence between a_{ef} and u_r , it is possible to estimate the time of arrival t from the roots of

$$1AU = u_r t + (1/2)a_{ef} t^2. \quad (3)$$

Figure 5 shows the travel time as a function of the corrected initial speed of the ejecta. The diamonds and the pluses indicate the observed τ and u_r for the same events in Figure 4. The solid line of Figure 5 corresponds to the solution of Eq. (3), assuming that a_{ef} is given by the parameters fitted when data from PVO-Helios1 are used (Gopalswamy *et al.*, 2002). The dashed line is obtained using $a_{ef} = -0.0042u_r + 1.79$ (the parameters obtained in this paper from SOHO/Wind data).

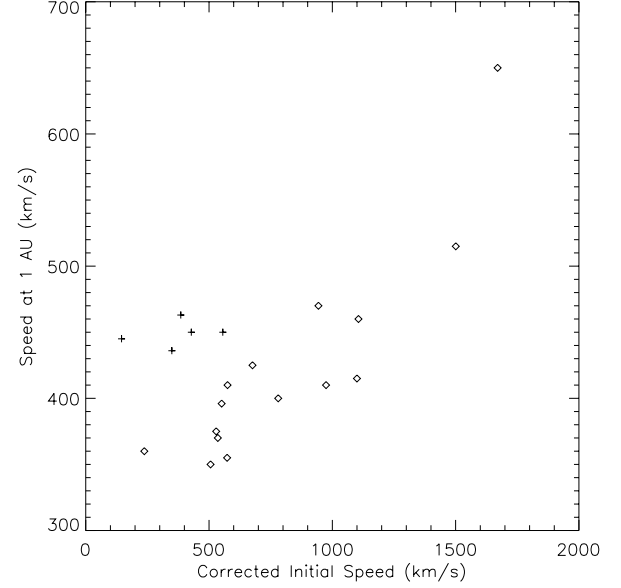


Fig. 4. Velocity of the ejecta, as observed *in situ* by Wind versus the radial speed of the CME. The plus signs correspond to events not correlated.

A recent work (Gopalswamy *et al.*, 2001) have shown that an acceleration cessation at distances $\sim 0.7AU$, is in reasonable agreement with the observations. Thus the dotted line corresponds to a model that consider two steps in the evolution of the CME, assuming that the acceleration is constant (and no null) up to 0.7AU followed by a free propagation (i.e., $a = 0$) beyond this distance.

The model curve in Figure 5 predicts an arrival time smaller than observed for most of the CMEs with corrected initial speeds >500 km/s. This must be due to the assumption we made that all the CMEs have the same initial width and that the measured sky plane speed is exactly the projected speed. In reality, both the assumptions may not be correct. CMEs show a broad distribution of widths. In addition to the radial motion, CMEs may also expand in the coronagraphic field of view. If this is so, then we may be overestimating the initial radial speed. In fact we see in Figure 5 that most of the data points are located to the right of the prediction curve, which might result from an overestimate of the initial radial speed. Gopalswamy *et al.* (2001) have discussed this issue in detail and suggest that while projection correction is important, there is no easy way of correcting for them.

Similar χ^2 tests are obtained for the three curves of Figure 5: 0.168, 0.180, and 0.184 days for dotted, solid, and dashed lines, respectively. These three last tests give a slightly better result when compared with the uncorrected speeds (and the correspondent model) are considered: 0.201 days.

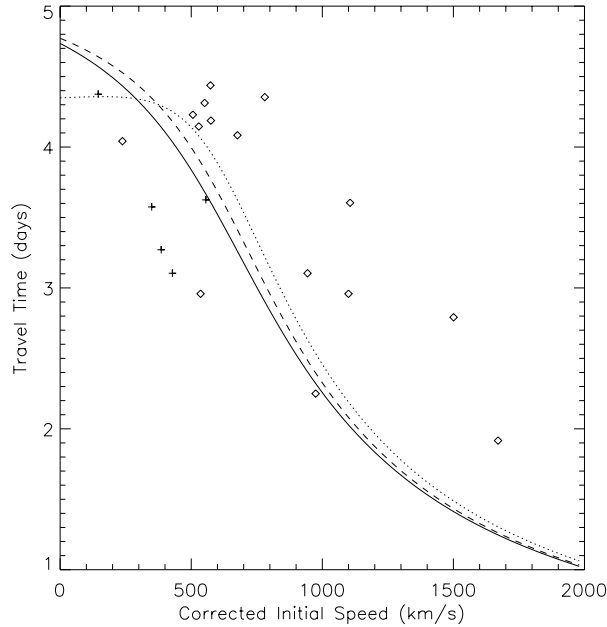


Fig. 5. Time of travel of the CME from the Sun's surface to 1AU. Rhombuses and plus signs correspond to the same events shown in Figure 4. The solid and dashed lines correspond to consider constant acceleration using the PVO-Helios1's parameters and the parameters obtained in this work, respectively. The dotted curve corresponds to a model considering acceleration constant up to 0.7 AU, and then a free motion.

CONCLUSIONS

In this paper we have analyzed the subset of the CMEs considered in (Gopalswamy *et al.*, 2000) and we corrected the speeds measured by SOHO/LASCO in the plane of the sky in order to obtain the radial velocity of the CME when it leaves the Sun surface.

We have shown that the corrections of the speed on the plane of the sky are very significant (reaching 70% of the observed velocity). This result expresses the necessity of carry out this correction in order to make better space weather predictions, with observations along the Sun-Earth line.

We have explored several different criteria in order to assign values to the semi-angle of the cone (α_r). However, the results are almost not sensitive to the chosen criterion, and all the results are very similar to that, which we choose to present in detail in this paper, i.e., $\alpha_r = 45^\circ$ for the whole set of CMEs studied.

The corrected initial speeds show a linear dependence with the effective acceleration ($a_{ef} = mu_r + b$). The values of m and b obtained in this work are very similar to that obtained, in a way completely independent, from PVO-Helios1

(Gopalswamy *et al.*, 2002), which do not need any correction, because they were obtained when both spacecrafts were in quadrature.

Prediction of the time of travel, using models with constant acceleration, are compared with the data. A χ^2 test is lightly better when the corrected speeds are used, against the uncorrected.

However, we expect that more realistic and sophisticated models (for instance, considering the acceleration as proportional to the speed) can provide better forecast to the arrival of CMEs.

Future observations from the STEREO mission (in quadrature with Earth), may be able to help us improve the results obtained in this paper.

ACKNOWLEDGMENTS

This work was partially supported by the Argentinean UBA (grant UBACYT X059).

BIBLIOGRAPHY

- AKASOFU, S. I., 1981. Energy coupling between the solar wind and the magnetosphere. *Space Sci. Rev.*, 28, 121-190.
- BURLAGA, L. F., E. SITTLER, F. MARIANI and R. SCHWENN, 1981. *J. Geophys. Res.*, 86, 6673.
- BURLAGA, L. G., 1995. *Interplanetary Magnetohydrodynamics*, Oxford Univ. Press, New York.
- CANE, H. V., I. G. RICHARDSON and O. C. ST. CYR, 2000. Coronal mass ejections, interplanetary ejecta and geomagnetic storms. *Geophys. Res. Lett.*, 27, 21, 3591-3594.
- CARGILL, P. J., J. CHEN, D. S. SPICER and S. T. ZALESK, 1995. Geometry of interplanetary magnetic clouds. *Geophys. Res. Lett.*, 22, 5, 647-650.
- CHEN, J., 1997. *In: Coronal Mass Ejections*, edited by N. Crooker, J. A. Joselyn, and J. Feynman, pp. 65, *Geophysical Monograph 99*, AGU, Washington, D. C.
- DUNGEY, J. W., 1961. Interplanetary magnetic field and the auroral zones. *Phys. Rev. Lett.*, 6, 47.
- FARRUGIA, C. J., L. F. BURLAGA, V. A. OSHEROVICH, I. G., RICHARDSON, M. P. FREEMAN, R. P.

- LEPPING and A. J. LAZARUS, 1993. A study of an expanding interplanetary magnetic cloud and its interaction with the Earth's magnetosphere: the interplanetary aspect. *J. Geophys. Res.*, 98, 7621-7633.
 - GONZALEZ, A. L. CLUA DE and W. D. GONZALEZ, 1998. Analytical study of the energy rate balance equation for the magnetospheric storm-ring current. *Annales Geophysicae*, 16, 1445-1454.
 - GONZALEZ, W. D., J. A. JOSELYN, Y. KAMIDE, H. W. KROEHL, G. ROSTOKER, B. T. TSURUTANI and V. M. VASYLIUNAS, 1994. What is a geomagnetic storm? *J. Geophys. Res.*, 99, 5771-5792.
 - GOPALSWAMY, N., A. LARA, R. P. LEPPING, M. L. KAISER, D. BERDICHEVSKY and O. C. ST. CYR, 2000. Interplanetary acceleration of coronal mass ejections. *Geophys. Res. Lett.*, 27, 2, 145-148.
 - GOPALSWAMY, N., A. LARA, S. YASHIRO, M. L. KAISER and R. A. HOWARD, 2001. Predicting the 1 AU arrival time of coronal mass ejections. *J. Geophys. Res.*, 106, 29207-29217.
 - GOPALSWAMY, N., 2002. Space weather study using combined coronagraphic and *in situ* observations, Space Weather Study Using Multipoint Techniques, Ed. by Ling-Hsiao Lyu, Pergamon Press, 39.
 - LEBLANC, Y., G. A. DULK, A. VOURLIDAS and J.-L. BOUGERET, 2001. Tracing shock waves from the corona to 1AU: Type II radio emission and relationship with CMEs. *J. Geophys. Res.*, 106, 25301-25312.
 - OSHEROVICH, V. A., C. J. FARRUGIA and L. F. BURLAGA, 1993. Dynamics of aging magnetic clouds. *Adv. Space Res.*, 13, 6, 57-62.
 - SHEELEY, N. R. JR., J. H. WALTERS, Y.-M. WANG and R. A. HOWARD, 1999. Continuous tracking of coronal outflows: Two kinds of coronal mass ejections. *J. Geophys. Res.*, 104, 24739-24767.
 - ST. CYR, O. C., R. A. HOWARD, N. R. SHEELEY JR., S. P. PLUNKETT, D. J. MICHEL, S. E. PASWATERS, M. J. KOOMEN, G. M. SIMNETT, B. J. THOMPSON, J. B. GURMAN, R. SCHWENN, D. F. WEBB, E. HILDNER and L. LAMY, 2000. Properties of coronal mass ejections: SOHO LASCO observations from January 1996 to June 1998. *J. Geophys. Res.*, 105, 18169-18185.
 - YEH T., 1995. A dynamical model of magnetic clouds. *ApJ*, 438, 975-984.
-
- S. Dasso^{1,2}, N. Gopalswamy¹ and A. Lara³
¹ NASA/Goddard Space Flight Center, Greenbelt, MD, and Center for Solar Physics and Space Weather, The Catholic University of America, Washington D.C, USA.
² Present Address: Instituto de Astronomía y Física del Espacio (IAFE), CC. 67 Suc. 28, 1428 Buenos Aires, Argentina
Email: dasso@df.uba.ar
³ Instituto de Geofísica, UNAM, México.